HYDROGEN, FUEL CELL & ENERGY STORAGE

Parametric Study of an ORC-EJR Cycle Based on Energy and Exergy Analysis for Power, Heating, Cooling, and Hydrogen Production

Ahmed Raad Ali Al-Aayedi[a] | **Morteza Khalilian**[a] | **Ata Chitsaz**[a]
Iraj Mirzaee[a,*] | **Hassan Shirvani**[b]

[a] Mechanical Engineering Department, Faculty of Engineering, Urmia University, Urmia, Iran
[b] Faculty of Science and Engineering, Anglia Ruskin University, Chelmsford, UK
[*] Corresponding author, Email: i.mirzaee@urmia.ac.ir

Article Information

Article Type
Research Article

Article History
Received: *10 Dec 2024*
Revised: *12 Feb 2025*
Accepted: *02 Mar 2025*
Published Online: *04 Mar 2025*

Keywords
Geothermal energy
Thermodynamic analysis
Hydrogen production
ORC-EJR

Abstract

Due to the environmental harm caused by fossil fuels and their limited availability, renewable resources have emerged as a viable alternative, driving extensive research in this field in recent years. Moreover, the adoption of integrated systems for power, cooling, heating, and hydrogen production has gained attention as an effective strategy to optimize the use of existing energy resources. In this study, a novel multigeneration system utilizing geothermal energy is introduced, with its performance modeled and analyzed. This innovative system integrates an ejector refrigeration cycle, an organic Rankine cycle, a local water heating unit, and a hydrogen generation system. The effects of various factors on the system's efficiency have been thoroughly examined. The results show that the system achieves energetic and exergetic efficiencies of 49.68% and 48.01%, respectively. The combined power output generated by the ORC turbine and a TEG is 499.89 kW. Additionally, the system produces a total of 166.9 kg of hydrogen daily, with a coefficient of performance (COP) of 0.355. Moreover, increasing the temperature of the geothermal fluid improves the exergetic efficiency, power generation, hydrogen production, and cooling load, while it reduces both the energetic efficiency and COP. Finally, it is concluded that increasing the geothermal mass flow rate leads to higher power generation, increased hydrogen production, a larger cooling load, and a decrease in both energy and exergy efficiencies.

Cite this article: Al-Aayedi, A. R. A., Khalilian, M., Chitsaz, A., Mirzaee, I., Shirvani, H., (2025). Parametric Study of an ORC-EJR Cycle Based on Energy and Exergy Analysis for Power, Heating, Cooling, and Hydrogen Production. DOI: 10.22104/hfe.2025.7274.1333

 Publisher: Iranian Research Organization for Science and Technology (IROST)
DOI: 10.22104/hfe.2025.7274.1333

1 Introduction

The global adoption of renewable energy sources is on the rise, driven by the diminishing availability of fossil fuels and the pollution and greenhouse gas emissions resulting from their combustion. To significantly increase the use of renewable energy, substantial technological and infrastructural changes are necessary. These changes include reducing energy consumption on the demand side, improving energy production efficiency, and replacing fossil fuels with various renewable energy sources [1]. Hydrogen energy presents a promising solution for the future, as hydrogen generated from renewable resources can significantly reduce environmental emissions [2, 3]. Research on hydrogen is vast, with many viewing it the key to future energy solutions. Hydrogen serves as an energy carrier, capable of storing and delivering energy in a usable form. However, it must be extracted from compounds that contain it [4,5]. Hydrogen can be generated from a variety of local resources, including fossil fuels such as coal (when paired with carbon capture) and natural gas, along with nuclear energy, biomass, and various renewable energy sources like wind, geothermal, solar, and hydroelectric power [6]. Numerous researchers have explored the integration of renewable energy sources into various systems for the generation of hydrogen and other products. Huang et al. [7] investigated a combined power and cooling system incorporating a Brayton cycle, an ejector refrigeration cycle, and an organic Rankine cycle, designed to utilize the waste heat from the exhaust gases and jacket water of combustion engines. Their results showed that the system achieves a net output power of 374.37 kW, a cooling capacity of 188.63 kW, and an exergy efficiency of 37.31%.

Boyaghchi et al. [8] analyzed a hybrid system utilizing a combination of solar and geothermal energy sources, focusing on its energy performance. The most effective solar configuration incorporated a storage tank and employed copper oxide nanofluid. Their findings revealed that the maximum energy efficiency and exergy efficiency for the R134a working fluid were 52.058% and 3.19%, respectively. Additionally, the study identified the minimum heat exchanger requirement for the R423A working fluid. Wang et al. [9] examined a proposed system that combines biomass and solar energy sources. The performance of this integrated system was evaluated using thermodynamic principles and environmental considerations. The results revealed that the biomass-driven system achieves superior energy efficiency and exergy output compared to the solar energy-driven system. On the other hand, the use of solar energy sources can play a crucial role in reducing greenhouse gas emissions. Anatone et al. [10] explored an innovative combined heating, cooling, and power (CCHP) system designed to leverage geothermal energy for minimizing greenhouse gas emissions. This advanced CCHP system integrates an internal combustion engine with a combined absorption heat pump, making it particularly suitable for small residential communities. Their study included an economic and environmental assessment of the system. The findings revealed a maximum cost reduction of 35% and a significant reduction in greenhouse gas emissions, reaching up to 60%.

Golafshani et al. [11] explored an innovative energy system integrating Photovoltaic Thermal (PVT) technology, which eliminates the reliance on batteries and heaters. The system employs ejector cooling, tailored for smart buildings capable of connecting to the power grid. The primary aim of this system is to reduce energy expenses for buildings by efficiently utilizing surplus electricity, which can be sold back to the grid. The findings reveal that the proposed system achieves an annual exergy efficiency of 21.98% with a low overall production cost of $22.48 per MWh. Under varying operating conditions, the system's annual exergy efficiency decreases to 14.18%, resulting in a total production cost of $34.01 per MWh. While numerous studies have focused on power and ejector refrigeration cycles individually, most have not thoroughly explored integrated power and ejector refrigeration systems. Therefore, this research examines a combined power-refrigeration cycle leveraging geothermal energy from a thermodynamic perspective.

2 System Description and Modeling

The diagram in Figure 1 depicts the multigeneration system under study. The proposed multigeneration cycle harnesses geothermal energy and consists of four integrated subsystems designed to produce power, cooling, heating, and hydrogen. These subsystems include an organic Rankine cycle, a domestic water heating system, an ejector refrigeration cycle, and a Proton Exchange Membrane (PEM) electrolyzer. Geothermal energy, a renewable resource, serves as the heat source for this cycle. Unlike conventional energy sources, renewables do not emit greenhouse gases, making them environmentally friendly. Harnessing geothermal energy offers both economic and environmental benefits by reducing pollution and providing a reliable, continuous energy supply.

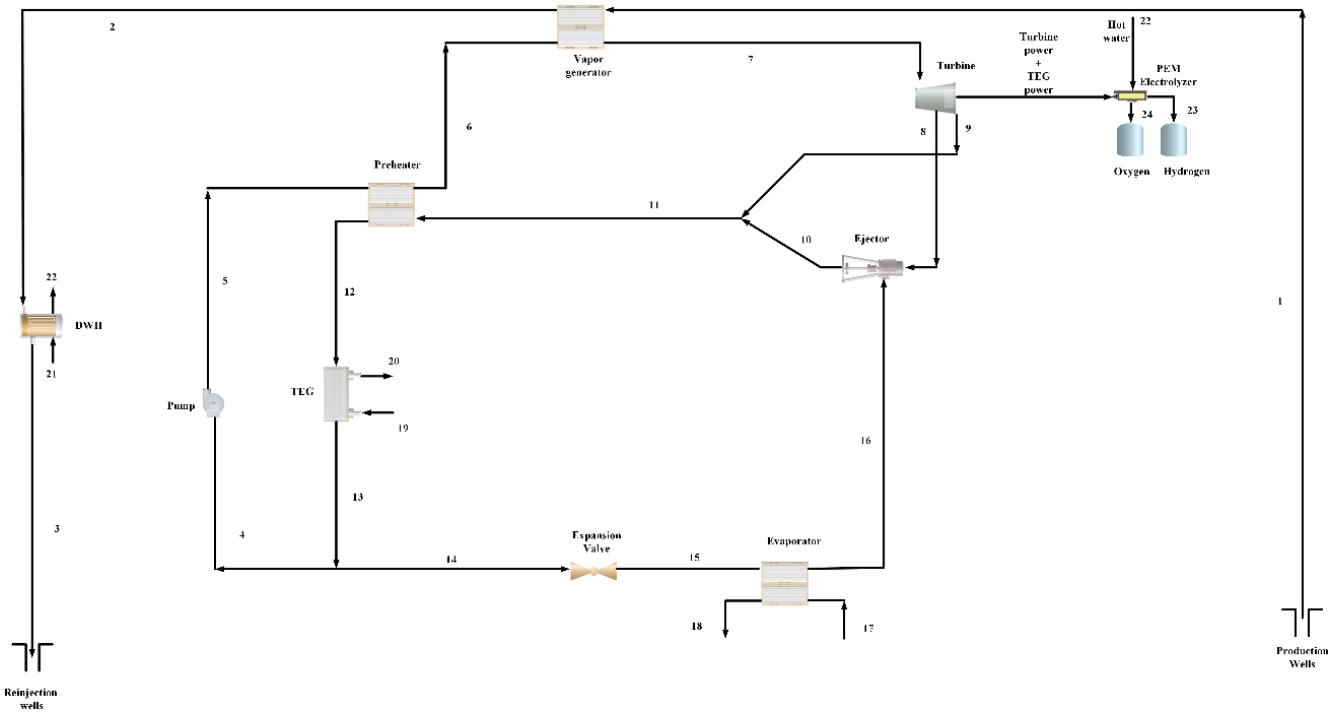

Fig. 1. Diagram illustrating the suggested geothermal multigeneration system

The following assumptions have been taken into account for modeling the proposed system:

- All flows within the system components are steady, and the pressure drops in the pipes as well as the heat losses to the surroundings within each component are disregarded.
- Changes in kinetic energy (except for the ejector modeling), as well as changes in potential and exergy energy, are neglected.
- Water serves as the geothermal heat source fluid.
- The output flows from the condenser and evaporator are assumed to be saturated liquid and saturated vapor, respectively.
- Isentropic efficiency is presumed for both the pump and the turbine.
- In the modeling of the ejector, the efficiencies of the diffuser, mixing section, and nozzle are taken into account.
- Ejector modeling is performed using constant pressure mixing.

The fundamental thermodynamic equations, including mass and energy balance equations for each system component, are presented below. The analysis is conducted using the Engineering Equation Solver (EES) software.

$$\sum \dot{m}_{\text{in}} - \dot{m}_{\text{out}} = \frac{dm_{cv}}{dt}\,, \tag{1}$$

$$\dot{Q} - \dot{W} + \sum_{\text{in}} \dot{m}_{\text{in}}\left(h_{\text{in}} + \frac{V_{\text{in}}^2}{2} + gZ_{\text{in}}\right) - \sum_{\text{out}} \dot{m}_{\text{out}}\left(h_{\text{out}} + \frac{V_{\text{out}}^2}{2} + gZ_{\text{out}}\right) = \frac{dE_{cv}}{dt}\,, \tag{2}$$

$$\dot{\text{E}}\text{x}_Q + \sum_{\text{in}} \dot{m}_{\text{in}}\text{ex}_{\text{in}} = \sum_{\text{out}} \dot{m}_{\text{out}}\text{ex}_{\text{out}} + \dot{\text{E}}\text{x}_W + \dot{\text{E}}\text{x}_D\,. \tag{3}$$

In the system's energy analysis, mass and energy balance equations are employed to determine thermodynamic properties such as temperature, pressure, enthalpy, entropy, and flow rates for all streams. After calculating these properties, the electrical output produced by various system components is evaluated. Table 1 presents the thermodynamic equations associated with each element of the proposed multigeneration system.

3 Results and Discussions

The accuracy of the calculations presented in Table 2 was validated in this study by comparing them with the findings of Wang et al. [12]. The results demonstrate a satisfactory level of agreement between the two, confirming their accuracy.

Table 1. Energy balance equations and the exergy destruction rate for every component of the proposed system.

Component	Energy balance equations	Exergy destruction rate equations
Vapor generator	$\dot{Q}_{\mathrm{vg}} = \dot{m}_1(h_1 - h_2) = \dot{m}_6(h_7 - h_6)$	$\dot{\mathrm{E}}\mathrm{x}_{d,\mathrm{vg}} = \dot{\mathrm{E}}\mathrm{x}_{d,\mathrm{vg}} = \dot{\mathrm{E}}\mathrm{x}_1 + \dot{\mathrm{E}}\mathrm{x}_6 - \dot{\mathrm{E}}\mathrm{x}_2 - \dot{\mathrm{E}}\mathrm{x}_7$
Turbine	$\dot{W}_t = (h_7 - h_8) + \dot{m}_9(h_8 - h_9)$	$\dot{\mathrm{E}}\mathrm{x}_{D,t} = \dot{\mathrm{E}}\mathrm{x}_7 - \dot{W}_t - \dot{\mathrm{E}}\mathrm{x}_8 - \dot{\mathrm{E}}\mathrm{x}_9$
Preheater	$\dot{Q}_{\mathrm{ph}} = \dot{m}_{11}(h_{11} - h_{12}) = \dot{m}_5(h_5 - h_6)$	$\dot{\mathrm{E}}\mathrm{x}_{\mathrm{ph}} = \dot{\mathrm{E}}\mathrm{x}_{11} + \dot{\mathrm{E}}\mathrm{x}_5 - \dot{\mathrm{E}}\mathrm{x}_{12} - \dot{\mathrm{E}}\mathrm{x}_6$
ORC TEG	$\dot{Q}_{\mathrm{TEG}} = \dot{m}_{12}(h_{12} - h_{13}) = \dot{m}_{19}(h_{20} - h_{19})$	$\dot{\mathrm{E}}\mathrm{x}_{D,\mathrm{TEG}} = \dot{\mathrm{E}}\mathrm{x}_{12} + \dot{\mathrm{E}}\mathrm{x}_{19} - \dot{\mathrm{E}}\mathrm{x}_{13} - \dot{\mathrm{E}}\mathrm{x}_{20}$
ORC pump	$\dot{W}_p = \dot{m}_4(h_5 - h_4)$	$\dot{\mathrm{E}}\mathrm{x}_{D,p} = \dot{W}_p - \dot{\mathrm{E}}\mathrm{x}_4 + \dot{\mathrm{E}}\mathrm{x}_5$
Evaporator	$\dot{Q}_{\mathrm{eva}} = \dot{m}_{15}(h_{16} - h_{15}) = \dot{m}_{17}(h_{18} - h_{17})$	$\dot{\mathrm{E}}\mathrm{x}_{d,\mathrm{eva}} = \dot{\mathrm{E}}\mathrm{x}_{15} + \dot{\mathrm{E}}\mathrm{x}_{17} - \dot{\mathrm{E}}\mathrm{x}_{16} - \dot{\mathrm{E}}\mathrm{x}_{18}$
Expansion valve	$h_{14} = h_{15}$	$\dot{\mathrm{E}}\mathrm{x}_{D,\mathrm{exv}} = \dot{\mathrm{E}}\mathrm{x}_{15} - \dot{\mathrm{E}}\mathrm{x}_{14}$
Ejector	-	$\dot{\mathrm{E}}\mathrm{x}_{D,\mathrm{eje}} = \dot{\mathrm{E}}\mathrm{x}_8 + \dot{\mathrm{E}}\mathrm{x}_{16} - \dot{\mathrm{E}}\mathrm{x}_{10}$
PEM	$\dot{W}_{\mathrm{PEM}} = \dot{m}_{22}h_{22} - \dot{m}_{23}h_{23} - \dot{m}_{24}h_{24}$	$\dot{\mathrm{E}}\mathrm{x}_{D,\mathrm{PEM}} = \dot{\mathrm{E}}\mathrm{x}_{22} + \dot{W}_{\mathrm{PEM}} - \dot{\mathrm{E}}\mathrm{x}_{23} - \dot{\mathrm{E}}\mathrm{x}_{24}$
DWH	$\dot{Q}_{\mathrm{DWH}} = \dot{m}_2(h_2 - h_3) = \dot{m}_{21}(h_{22} - h_{21})$	$\dot{\mathrm{E}}\mathrm{x}_{\mathrm{DWH}} = \dot{\mathrm{E}}\mathrm{x}_2 + \dot{\mathrm{E}}\mathrm{x}_{21} - \dot{\mathrm{E}}\mathrm{x}_3 - \dot{\mathrm{E}}\mathrm{x}_{22}$
COP	$\mathrm{COP} = \dfrac{\dot{Q}_{\mathrm{eva}}}{\dot{Q}_{\mathrm{vg}} + \dot{W}_P}$	

Table 2. Comparison of the current study's findings with the reference's findings [12].

Parameter	Current study	Ref [12]	Difference
Turbine power (kW)	114.14	116.47	2.04
Pump power (kW)	3.45	3.49	1.16
Cooling effect (kW)	60.44	60.51	0.11
Boiler heat transfer (kW)	1246.96	1276.35	2.35
Total exergy destruction rate (kW)	334.42	336.86	0.73
Thermal efficiency (%)	13.72	13.61	0.8
Exergetic efficiency (%)	22.2	22.41	0.94

Table 3. The general simulation results for the proposed system for two different solar collectors.

Parameters	Value
η_{en} (%)	49.68
η_{ex} (%)	48.01
$\dot{W}_{t,\mathrm{ORC}}$ (kW)	411.5
$\dot{W}_{\mathrm{TEG}}$ (kW)	88.39
$\dot{W}_{\mathrm{net,ORC}}$ (kW)	499.89
COP	0.355
Q_{cooling} (kW)	1398
$\dot{m}_{\mathrm{H_2}}$ (kg/day)	166.9
$\dot{\mathrm{E}}\mathrm{x}_{d,\mathrm{tot}}$ (kW)	4379
Z ($)	47197

To conduct the analysis, thermodynamic laws were applied, and energy and exergy balance equations were formulated for the various components of the system. These governing equations and relationships were derived for each part of the system. Subsequently, the system's performance was simulated and analyzed using EES software. Table 3 presents the results related to the operational characteristics of the proposed multi-generation system, comparing its performance with different types of solar collectors.

Based on the overall analysis, the system achieves energy and exergy efficiencies of 70.97% and 48.01%, respectively. The refrigeration system produces a cooling effect of 1398 kW with a coefficient of performance (COP) of 0.355. Additionally, the thermoelectric generator (TEG) unit contributes 88.39 kW of power, complementing the 411.5 kW generated by the turbine. Finally, the results indicate that the system is capable of producing 166.9 kg of hydrogen per day.

Figure 2 illustrates the relationship between the geothermal fluid temperature and the system's energy and exergy efficiencies. The results show an inverse relationship: as the geothermal temperature increases, the system's energy efficiency decreases while its exergy efficiency increases. Specifically, when the geothermal temperature rises from 425 K to 450 K, the energy effi-

ciency decreases from 61.47% to 49.51%, while the exergy efficiency increases from 43.58% to 48.03%. This decline in energy efficiency occurs because the energy produced by the vapor generator and transferred to the bottoming system exceeds the power generated by the system at higher geothermal temperatures.

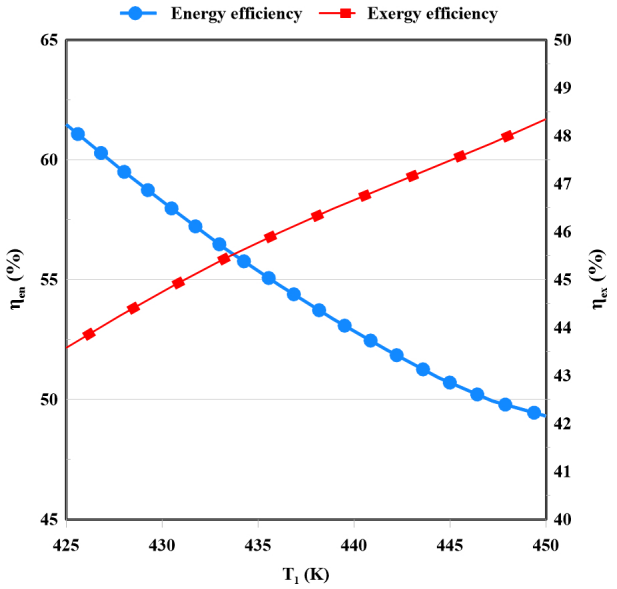

Fig. 2. The impact of the geothermal fluid temperature on the energy and exergy efficiency of the system.

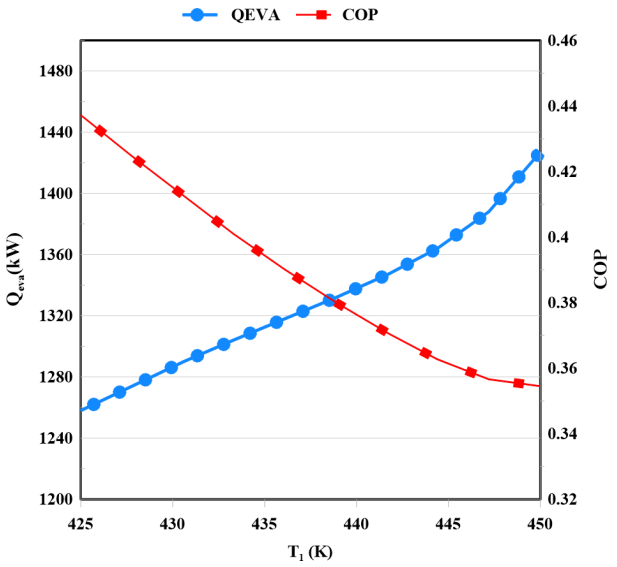

Fig. 3. The impact of geothermal fluid temperature on both the cooling load and the system's COP.

Figure 3 shows the relationship between the geothermal fluid temperature and the system's cooling load and coefficient of performance (COP). The results indicate that as the geothermal fluid temperature increases, the system's cooling load increases while its COP decreases. Specifically, when the temperature is raised from 425 K to 450 K, the COP drops from 0.437 to 0.354, while the cooling load increases from 1258 kW to 1427 kW. This decrease in COP occurs because an increase in geothermal temperature raises both the cooling effect generated in the evaporator and the heat produced in the vapor generator. However, the heat generated in the vapor generator exceeds the cooling effect, leading to a decline in COP.

Figure 4 illustrates the impact of geothermal water temperature on the system's power and hydrogen generation outputs. The results show that as the geothermal fluid temperature increases, both power and hydrogen generation rates also increase. An increase in the geothermal source temperature leads to a corresponding rise in the turbine inlet temperature, while a decrease in the geothermal temperature results in a lower turbine inlet temperature. Higher turbine inlet temperatures lead to increased enthalpy, which enhances the difference between the enthalpy at the turbine's inlet and outlet, thereby boosting the turbine's output power.. The turbine, along with the TEG unit, provides energy to the PEM electrolyzer, which is essential for hydrogen production. As a result, an increase in turbine-generated power leads to a higher hydrogen production rate.

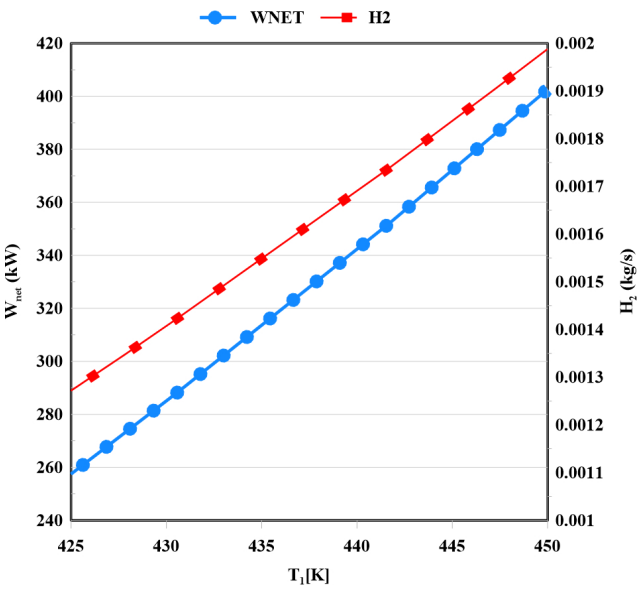

Fig. 4. The influence of the temperature of the geothermal fluid on the quantity of power and hydrogen produced by the system.

Figure 5 shows the relationship between the system's energy and exergy efficiency and the mass flow rate of the geothermal fluid. The results show that as the mass flow rate increases, both energy and exergy efficiencies decrease. Specifically, energy efficiency de-

creases from 49.99% to 49.57%, and exergy efficiency decreases from 50.73% to 47.1% as the mass flow rate increases from 5 kg/s to 15 kg/s. An increase in the mass flow rate of the geothermal fluid results in a greater amount of energy being transferred to the ORC-EJR cycle from the vapor generator. Furthermore, the system's power output increases. However, because the heat transfer ratio in the vapor generator to the output power exceeds 1, the overall efficiency of the system decreases.

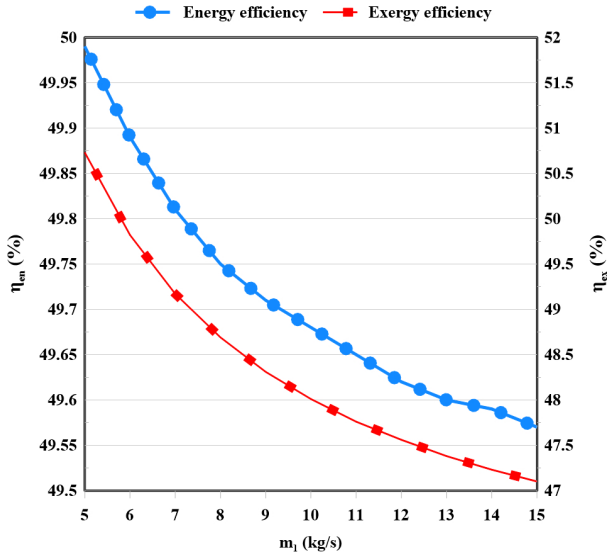

Fig. 5. The effect of the mass flow rate of the geothermal fluid on the energy and exergy efficiency of the system.

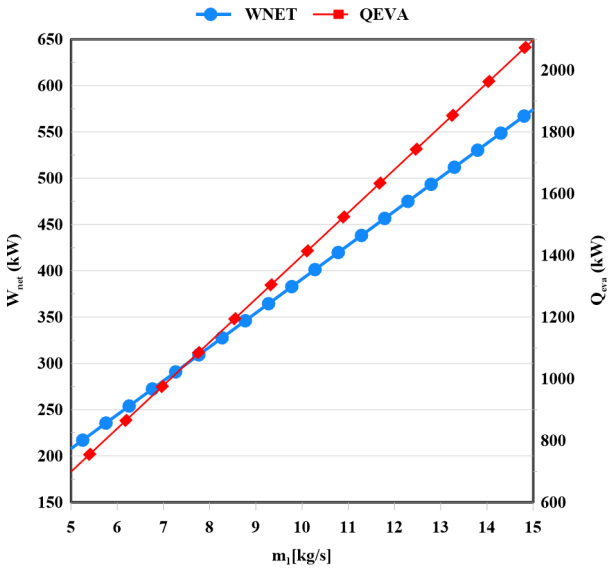

Fig. 6. The influence of the geothermal fluid mass flow rate on the levels of power generation and the system's cooling demand.

The effect of the geothermal fluid mass flow rate on power production and the system's cooling load is illustrated in Figure 6. The graphs indicate that as the mass flow rate increases, both the power output and the cooling load produced in the evaporator rise. Specifically, increasing the mass flow rate from 5 kg/s to 15 kg/s results in the power output increasing from 207.9 kW to 574.3 kW, while the cooling load in the evaporator increases from 699.2 kW to 2098 kW. As the geothermal mass flow rate increases, additional energy is transferred to the ORC-EJR cycle, leading to enhanced power and cooling load generation.

Figure 7 illustrates the effect of the geothermal fluid mass flow rate on the hydrogen production rate. As the mass flow rate of the geothermal fluid increases, the hydrogen production rate rises from 0.001026 kg/s to 0.002836 kg/s. The PEM electrolyzer, which is responsible for hydrogen production within the system, receives energy from both the turbine and the TEG unit. An increase in the geothermal mass flow rate enhances the overall power generation of the system, leading to higher hydrogen production rates.

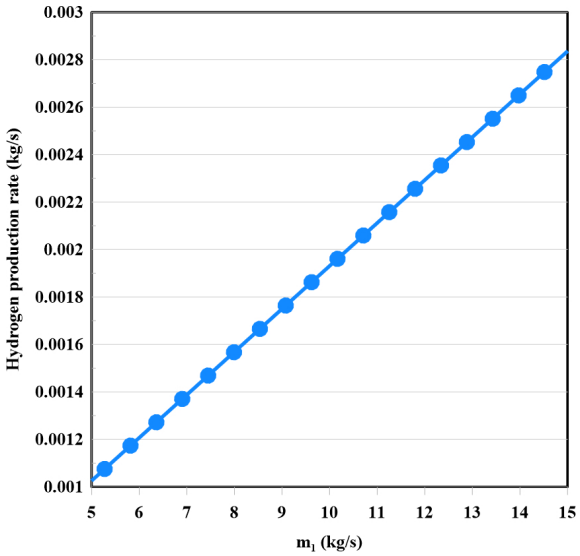

Fig. 7. The effect of the mass flow rate of geothermal fluid on the rate of hydrogen production.

Figure 8 illustrates the impact of using different working fluids in the ORC-EJR cycle on the system's efficiency. A total of five working fluids – R132, R141b, R245fa, R600, and R600a – are analyzed to evaluate their performance. Typically, as the temperature of the geothermal fluid increases, the energy efficiency of all working fluids improves. The findings indicate that, among the five working fluids analyzed, R600a demonstrates the highest energy efficiency, while R600 exhibits the lowest. Specifically, for R600a, the energy efficiency ranges from 15.63% to 16.66%, while for R600, it ranges from 10.21% to 10.88%, as the geothermal

fluid temperature increases from 425 K to 450 K.

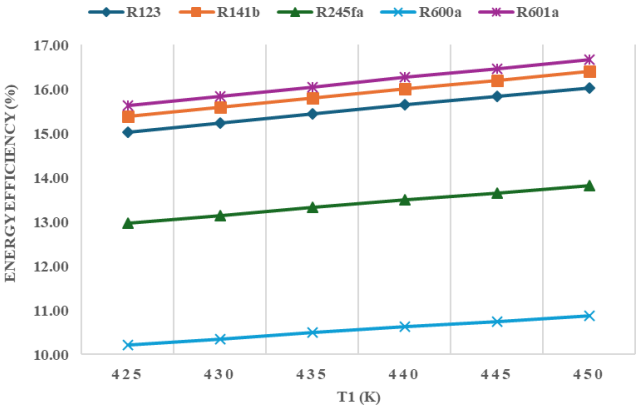

Fig. 8. The impact of various working fluids on the system's energy efficiency.

Figure 9 compares the power generated by the ORC turbine and the TEG unit. The results show that the ORC turbine generates 411.5 kW, while the TEG unit produces 88.39 kW. This means that the ORC turbine contributes 78.6% of the total power generated by the system, and the TEG unit contributes 21.4%. The figure highlights that by replacing the condenser with the TEG unit in the system, an additional 21.4% of power can be produced without relying on any external energy source.

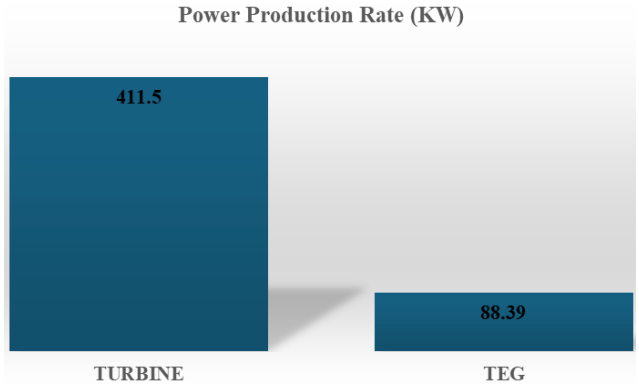

Fig. 9. Comparison of power generation rate by the turbine and the TEG.

4 Conclusions

This study introduces and examines an innovative multigeneration cycle (ORC-EJR) that integrates an ejector refrigeration cycle with the organic Rankine cycle, focusing on both thermodynamic and thermoeconomic aspects. The system is designed to generate hydrogen, heat, electricity, and cooling. Geothermal energy serves as a sustainable power source in this proposed configuration. By utilizing renewable energy, energy waste can be minimized, and multiple outputs can be produced at a low cost. Additionally, the system's condenser is substituted with a thermoelectric generator (TEG) unit to generate additional electricity. The analysis of various parameters leads to the following conclusions.

- The system demonstrates energy and exergy efficiencies of 49.68% and 48.01%, respectively.
- The overall power output produced by the system via the ORC turbine and a single TEG amounts to 499.89 kW.
- This system produces a total of 166.9 kg of hydrogen on a daily basis.
- The coefficient of performance (COP) for this system has been recorded at 0.355.
- Raising the temperature of the geothermal fluid improves the exergetic efficiency, power output, hydrogen yield, and cooling load of the system, while it reduces energetic efficiency and the COP.
- An increase in the geothermal mass flow rate leads to greater power generation, higher hydrogen production rates, an augmented cooling load in the system, while simultaneously decreasing both energy and exergy efficiency.

References

[1] Lund H, Mathiesen BV. Energy system analysis of 100% renewable energy systems—The case of Denmark in years 2030 and 2050. Energy. 2009;34(5):524–531.

[2] Midilli A, Dincer I. Key strategies of hydrogen energy systems for sustainability. International Journal of Hydrogen Energy. 2007;32(5):511–524.

[3] Yilanci A, Dincer I, Ozturk HK. A review on solar-hydrogen/fuel cell hybrid energy systems for stationary applications. Progress in energy and combustion science. 2009;35(3):231–244.

[4] Berry GD, Pasternak AD, Rambach GD, Smith JR, Schock RN. Hydrogen as a future transportation fuel. Energy. 1996;21(4):289–303.

[5] Cohce M, Dincer I, Rosen M. Thermodynamic analysis of hydrogen production from biomass gasification. International Journal of Hydrogen Energy. 2010;35(10):4970–4980.

[6] Momirlan M, Veziroglu TN. The properties of hydrogen as fuel tomorrow in sustainable energy system for a cleaner planet. International journal of hydrogen energy. 2005;30(7):795–802.

[7] Huang W, Wang J, Xia J, Zhao P, Dai Y. Performance analysis and optimization of a combined

cooling and power system using low boiling point working fluid driven by engine waste heat. Energy Conversion and Management. 2019;180:962–976.

[8] Boyaghchi FA, Chavoshi M, Sabeti V. Optimization of a novel combined cooling, heating and power cycle driven by geothermal and solar energies using the water/CuO (copper oxide) nanofluid. Energy. 2015;91:685–699.

[9] Wang J, Yang Y. Energy, exergy and environmental analysis of a hybrid combined cooling heating and power system utilizing biomass and solar energy. Energy Conversion and Management. 2016;124:566–577.

[10] Anatone M, Panone V. A model for the optimal management of a CCHP plant. Energy Procedia. 2015;81:399–411.

[11] Golafshani SR, Fatehpour M, Houshfar E. Optimization and dynamic techno-economic assessment of integrated combined ejector cooling, heating, and power system. Energy. 2023;282:128829.

[12] Dai Y, Wang J, Gao L. Exergy analysis, parametric analysis and optimization for a novel combined power and ejector refrigeration cycle. applied thermal engineering. 2009;29(10):1983–1990.